SCA-9934

GAS/OIL RELATIVE PERMEABILITY CURVES

FOR DEEP WATER RESERVOIRS

G. Hamon, F. Gouth, P. Bergey, D. Gaujard

Elf Exploration Production

ABSTRACT :

The deep water reservoirs are increasing areas of activities for the oil industry. The reinjection of produced gas in these high permeability, unconsolidated sands is an important issue. In the case of immiscible displacements, the success hinges on the efficiency of gas/oil gravity drainage. Critical factors are reservoir heterogeneity, vertical permeability and gas-oil relative permeability curves. This paper addresses several issues associated with gas/oil relative permeability curves.

1. Firstly, this paper illustrates some techniques carried out to ensure the quality and integrity of the totally unconsolidated samples. Several features are described : a) a new sample sleeve which eliminates sand disturbance during core flood sample coring and ensures a very good control of radial strain during sample loading up to the reservoir effective stress. b) a cheap core flood test to discard heterogeneous samples once in the core holder and prior to the gas flooding test
2. Secondly, this work also illustrates some key features of the determination of gas/oil relative permeability curves, especially important on the shape of the oil relative permeability curve and the " residual " oil saturation such as multi-rate gas flood used in combination with inversion methodology.
3. Thirdly, this paper describes the approach performed to relate gas/oil relative permeability curves lithology, using macrolithological descriptions, grain size analysis, X-Ray diffraction
4. In-house gas/oil data set was reviewed for one reservoir and trends between gas/oil Kr and other petrophysical parameters were sought. Grain size distribution was found to control both the shape of the oil relative permeability and residual oil saturations.
5. This work also describes the approach used to populate the 3D reservoir models with gas/oil relative permeability, taking into account the grain size distribution. The sensitivity of production forecasts is also shown.

INTRODUCTION

The deep water reservoirs are increasing areas of activities for the oil industry. All experimental results presented in this paper were obtained on samples from deep offshore fields A and B. The main reservoirs consist of totally unconsolidated, highly permeable, massive turbidite sands.

Gas re injection is necessary to avoid flaring and to remedy the lack of gas disposal or gas utilization facilities in the vicinity. Among the various reservoirs present in field B, one is thought as being the best candidate for gas injection (lowest potential reserves losses associated with gas injection). This reservoir can be described as being of low NTG / fairly layered in the upper and mid sequences, and made of quite homogeneous massive sand in the lower sequence (over 50 meters). The poor top and mid zones can help to delay gas breakthrough while the lower sequence allows a good gravity drainage, whose efficiency depends a lot on permeability level and oil relative permeability curve shape. Gas injection would be performed at the top and would aim at ensuring the pressure maintenance, horizontal producers being therefore placed at the very bottom of the oil column

Initial pressure and temperature conditions, as well as crude oil properties result in immiscible gas/oil displacements. The very high permeabilities are favourable for a gravity-stable gas displacement provided that reservoir structure and heterogeneity do not result in poor areal sweep

It has long been evidenced that relative permeability to oil is a key factor in the gas/oil gravity drainage. Pessimistic Krog curves lead to poor microscopic recovery whereas little oil can be left behind with more favourable curves.

To ensure the gas/oil relative permeability curves obtained on high permeability, unconsolidated samples are reliable, several steps in the core selection, core handling and core flood design have been revisited. This paper addresses several issues of the experimental work such as the homogeneity of the samples, accounting for a capillary end-effect during flood experiments and simultaneous determination of relative permeabilities and capillary pressure curves.

Once relative permeability curves have been obtained from a large number of samples, there is often a significant scatter in results. This paper also presents an integrated approach to assign gas/oil relative permeability curves to a fine grid reservoir model for a deep water unconsolidated reservoir

CORE QUALITY AND INTEGRITY

It is agreed that small-scale heterogeneities can have a severe effect on two-phase flow and can result in erroneous interpretations of core floods (Hamon, 1986 ; Huang, 1994 ; Sylte, 1998). Several types of measurements are routinely performed to select the most homogeneous but representative consolidated samples used for core flooding tests : closely spaced minipermeameter measurements (Dauba, 1998), 3D computed tomography (CT) density, 1D X-Ray or Gamma-Ray profiles. On unconsolidated reservoirs however, core quality and integrity becomes a major issue:

- Cores are more prone to damage during the coring and core handling steps due to the very weak mechanical strength. Bit action, mud fluid invasion, pressure blowdown during the trip out of the well and core handling may disturb the core,
- Some simple and cheap techniques, such as probe permeameter, cannot be run on unconsolidated samples,

Consequently, check of homogeneity of poorly consolidated cores often hinges on CT scan and visual inspection only.

Firstly, CT Scan and visual inspection of whole-core samples is routinely performed to select the most homogeneous and the less disturbed parts of the cores. Secondly, CT scan inspection must be performed again on the sample plug to be used for core flood test as plug cutting and transfer into the sleeve may result in additional disturbance. Finally, the sample plug should be scanned again once mounted in the coreholder and loaded back to reservoir net effective stress as unconsolidated cores always show a strong response to the loading from initial low stress to in-situ stress.

Our experience shows that CT proved to be a very useful tool in delineating severely disturbed, layered, laminated or coarse gravel sections for sample selection. However we frequently observe that sections deemed homogeneous after the second CT inspection finally exhibit significant heterogeneities. This is particularly true for sections coming from the thick turbidite sands from field A and B. These weaknesses of CT scan inspection may be related to :

- Vertical gradients in grain-size distributions,
- Small scale heterogeneities originating from stress relief out of the wellbore: either differential deconsolidation or very small fissures along the sample. These features result in weak differences in CT density

Trends in grain-size distribution can be easily identified by grain-size analysis at both ends of any sample and sections including significant trends can be discarded. On the other hand, the detection of slightly deconsolidated zones from CT images is rather subjective and there was a need for an additional estimate of heterogeneity once the sample has been mounted in the coreholder and loaded to in-situ stress.

Tracer flow experiments :

Tracer flow experiments have often been reported and used in the past to compute a longitudinal dispersion coefficient using the convective-dispersive equation. This approach has often resulted in surprisingly large values which are, in fact, mainly caused by small-scale heterogeneity. This was confirmed by some research studies which illustrated that the output concentration may be much more sensitive to along-axis heterogeneities than dispersion (Sultan, 1987 ; Bahralolom, 1992). Recent techniques take advantage of the CT to image local flow patterns and compute local concentrations (Narayanan, 1988 ; Bahralolom, 1992). Although inversion of local concentration profiles might be an efficient method to get spatial distribution of petrophysical parameters, this technique is demanding more CT availability and computer resources than the simpler approach that we performed.

Our approach to ensure the integrity and homogeneity of unconsolidated samples is based on a combination of three types of information : 1) Brine/brine miscible tracer flow experiments, 2) qualitative CT scans inspection, 3) 1D X-Ray or Gamma-Ray profiles. This approach is fully described in a companion paper (SCA 9933 : Dauba, 1999), but is summarised hereafter.

Forward modelling has been extensively run for computing the sensitivity of the output tracer concentration curve to different types of small-scale heterogeneities and for generating effluent type-curves. These sensitivities were also very helpful for designing the tracer experiments as well as providing critical insights to the region of influence of rate, type of heterogeneity and permeability contrast. These type-curves, coupled with estimated geometry of heterogeneity from CT images form the basis of the identification of plug heterogeneities. This work illustrated that tracer flow experiments resolve channels to flow better than barriers to flow. For across- core axis heterogeneities, 1D X-Ray or Gamma-Ray profiles proved to be the best indicators.

Once a consistent response between geometry from CT scans and type of effluent curve has been established, the core is simplified to a two regions representation : a high and a low permeability region. Finally, history match of the experimental tracer concentration history is carried out with a 2D, fine grid numerical model incorporating both convection and dispersion to obtain a coarse estimate of the permeability contrast.

Step brine/brine tracer flow experiments have been routinely performed for the selection and a coarse estimate of permeability heterogeneity on dozens of samples of Field A and B. Figure 1 shows three experimental output tracer curves on unconsolidated sand samples. Sample 1 response is nearly symmetric about one pore volume and CT images confirm that the sample is very homogeneous. Concentration profile from sample 2 exhibits an early breakthrough and an extended concentration tail whereas sample 3 shows also a strong asymetry and a long tail. Such distorted effluent curves were not anticipated from the initial inspection of CT scans. Further detailed inspection of both along and across axis scans suggested a layer-cake model for sample 3 for instance as illustrated by Figure 1. This geometry was put in the 2D miscible flow model and did capture the key features of the effluent curves. The history match resulted in a permeability contrast between the two regions ranging between 5 and 10. The difference in effluent curves between samples 2 and 3 originates from the volumetric fraction of the high permeability region. Such a permeability layering can be put in a 2D two-phase flow simulator to history match the gas flood experimental results.

This approach was extensively used to disregard samples with large permeability contrast. Core flood tests on heterogeneous samples are avoided. Then, this combination of three types of information about small-scale heterogeneity usually prevents a waste of time and money.

Sample sleeve :

It has long been recognised that the in-situ stress in reservoirs is more correctly represented by zero lateral strain rather than hydrostatic stress conditions. These strain conditions are usually obtained through a " triaxial " loading, the axial stress being the maximum principal stress. In a " triaxial " loading, a uniform radial stress is applied by hydraulic pressure to the sample, and acts on a Viton membrane sheathing the core plug. This design works well when short plugs are cut under liquid nitrogen. However, it is always desirable to get the longest samples for core floods on very permeable samples to obtain a reliable value of the differential pressure. It is experienced that this design results on unexpected deformations during the loading phase of long or composite cores. Moreover, plug cut under liquid nitrogen may be inappropriate, for shaly sands for instance and the transfer of unconsolidated samples into a Viton sleeve may cause mechanical disturbance.

The innovation lies in a novel sample sleeve, composed of a composite of aluminium and rubber coating which is used to cut the plug and then mounted directly in the coreholder. This sleeve minimises strains during the plug cut, directly ensures the zero strain condition like in an oedometric cell when the sample is loaded to in-situ stress and is transparent to X-Rays or Gamma-Rays.

DETERMINATION OF GAS/OIL RELATIVE PERMEABILITY CURVES :

Design of gas core floods :

Drainage gas-liquid corefloods result in a significant capillary end-effect as gas is non-wetting (Delclaud, 1972, 1974). Several experimental or interpretation techniques were published to eliminate or minimise the capillary end-effect from coreflood tests (Jennings, 1988 ; Kohhedee, 1994, Hornarpour, 1988). In this work, the effect of capillary forces is not neglected but investigated through a dedicated test design : multi-rate unsteady-state gas flooding experiments coupled with a simultaneous determination of both relative permeability and capillary pressure curves are performed. This method does neither require a special experimental set-up nor simplifying assumptions.

During the gas flood, the injection rate or overall differential pressure is increased stepwise. At the lowest differential pressure, capillary forces result in a significant outlet end-effect. Each differential pressure increase :

- Changes the competition between viscous forces and resisting capillary forces :
- Results in a transient additional oil recovery curve until a new balance between viscous and capillary forces is reached (see figure 2).

The capillary end-effect is progressively squeezed out.
This multi-rate design has several advantages : the initial part of the gas flood experiment is carried out at relatively low flow rates but further changes in the balance between viscous and capillary forces are an advantage for the simultaneous determination of Kr and Pc curves. Finally, the last step at a high differential pressure ensures that the capillary end-effect has been minimised. Gas flooding experiments are performed with initial water saturation. Instantaneous gas and oil rates and overall differential pressure are recorded versus time throughout each rate step.

Interpretation of gas core floods :

Gas/oil relative permeability and capillary pressure curves are obtained simultaneously using a constrained weighted least squares optimisation. Numerous research works investigated the simultaneous determination of Kr and Pc curves (Chavent, 1980 ; Kerig, 1987 ; Richmond, 1990 ; Ucan , 1993 ; Nordtvedt, 1994)

This technique requires the minimisation of an objective function. The objective function is of the form : $J= J_1+J_2+J_3$ where J_1, J_2, J_3 are the contribution to J from the pressure drop, oil production and local saturation data, respectively.

J_1, J_2 are given by : $J_k = WT_k^2 . \sum_i wt_k(i)^2 . [Y_m(i) - Y_s(i)]^2$ where $Y_m(i)$ is the measured value of differential pressure (oil production) at a time t(i) and $Y_s(i)$ is the value of differential pressure (oil production) obtained at a time t(i) by a direct simulation using a 1D, black-oil, fully implicit core flood simulator which accounts for both capillary and gravity forces and appropriate boundary conditions.

In the same way, $J_3 = WT_3^2 . \sum_i wt_3(i)^2 . \left(\frac{1}{Nb_p} \right) . \sum_j (Y_m(i,j) - Y_s(i,j))^2$ where $Y_m(i,j), Y_s(i,j)$ are the measured (simulated) values of saturation at a time t_i at a position x_j in the core and Nb_p the number of points used to define the profile. WT_k. and wt_i are appropriate global and individual weighting factors.

The type of functional representation of relative permeability curves is known to be a key factor of the accuracy of parameter estimation methods. A modified cubic spline interpolation is used to ensure flexibility and to prevent oscillations in the interpolating function.

Uniqueness of results :

Several studies have addressed the issue of uniqueness in the determination of relative permeability and capillary pressure functions using an history match technique (Grimstad, 97 ; Ucan,97). Recent work concluded that both internal core data (saturation profiles), fluid production data and differential pressure must be used simultaneously for history matching to ensure the uniqueness (Ucan, 97). However, without incorporating saturation profiles in the history matching, the reliability of gas/oil relative permeability curves can be assessed if the drainage capillary pressure curve is known through an independent experiment. Figure 3 shows the comparison between :

- the numerical estimate of the drainage capillary pressure curve issued from simultaneous determination of Kr and Pc from multi-rate unsteady-state gas flood,
- experimental measurements of gas/oil drainage capillary pressure curves on unconsolidated sands,

The agreement is very good and confirms the reliability of the simultaneous determination of Kr and Pc from a single multi-rate gas flood, even when saturation profiles are not accounted for. Solution is not unique but the estimate is deemed accurate enough for reservoir engineering applications.

RESULTS

Oil relative permeability curve :

Early studies highlighted the importance of the curvature of the oil relative permeability curve on the recovery curve (Hagoort, 1980). A Corey-type exponential form will be used in this paper to compare the Krog curves obtained on the different samples from Field A and B,

$$S_{oD} = \frac{S_o}{1 - S_{wirr}} \text{ Equation 1} \qquad k_{rog} = A S_{oD}^{no} \text{ Equation 2} \qquad k_{rgo} = (1 - S_{oD})^{ng} \text{ Equation 3}$$

Inspection of oil relative permeability curves from Field A and B shows two different behaviours :

1. There is a break in the log/log plot of krog(So) at low oil saturations, as illustrated by sample A in figure 4:

   - In the high and medium oil saturation range, Krog(So) is best fitted by : $Krog(S_o) \propto S_{oD}^{no}$ with 3.7 < no < 6.5
   - In the low oil saturation range, Krog(So) is best fitted by : $Krog(S_o) \propto S_{oD}^{no}$ with 1.5 < no < 2.5

   This is the most represented behaviour.

2. There is no break in the log/log plot of krog(So) at low oil saturations, as illustrated by sample C in figure 5 : Krog(So) is best fitted by : $Krog(S_o) \propto S_{oD}^{no}$ with 3.7 < no < 6.5

The first behaviour is very favourable to gravity drainage as the oil relative permeability asymptotically extrapolates to zero residual oil saturation whereas the second behaviour leads to significant oil trapping : SoD=0.19 at Krog=1^{e-5} for some samples, see Figure 6.

Low residual oil saturations :

The concept of spreading of oil on water in the presence of gas was first used to explain the very low oil saturations obtained by gas gravity drainage in highly permeable sand packs (Dumoré, 1974). This was confirmed by gravity drainage experiments in consolidated and unconsolidated cores, visualisations in 2D micromodels (Chatzis, 1988 ; Kantzas a, b 1988) as well as corefloods on highly permeable reservoir cores (Delclaud, 1987). Several research works illustrated that gas/oil rel perms for primary drainage with connate water saturation depend on wettability and spreading (Vizika, 1996 ; DiCarlo, 1998). The largest oil recovery by gas injection are obtained for spreading conditions and water-wet or fractionally-wet rocks. Measurements of the three interfacial tensions used for Field A and B experiments confirm that the fluid system was spreading.

Quadratic form of oil relative permeability curve :

Our core floods measurements show that the oil exponent might range from 1.5 to 2.5 for low oil saturations. This is in agreement with recent results from gravity drainage experiments on a sand-pack for a spreading octane/brine/air system (Sahni, 1998).

This research work illustrated that $Kr_{og} \propto S_o^2$ in the low oil saturation range and $Kr_{og} \propto S_o^4$ in the high oil saturation range. Relative permeability was calculated directly from CT saturations. Oil film flow in spreading systems was the basis for the theoretical explanation of this quadratic form (Fenwick, 1998 ; Sahni, 1998). The slope variation in the log/log plot of krog(So) at low oil saturations observed on our samples might be ascribed to the change from bulk flow to film flow for spreading oils in three-phase conditions.

These results also confirm that an experimental Krog curve cannot be correctly represented by a Corey form with a single-adjustable parameter. It is our general experience. This also shows that interpretations of coreflood tests or parameter estimations methods which assume single-parameter exponential forms cannot reproduce correctly experimental data. In agreement with previous work (Kerig, 1986), these gas floods show that a representation using spline functions adds the required flexibility to capture this key behaviour.

The origin of two different behaviours in the low So region is still unclear as the same fluids were used for all samples and all gas floods were performed with connate water saturation.

Scatter in oil relative permeability curvatures :

There is a large scatter in oil relative permeability curves for fields A and B. The oil Corey exponent ranges from 3.7 to 6.5 in the high and medium oil saturation range, as illustrated by Figure 6. Such a scatter will result in large differences in the recovery curves by gas/oil gravity drainage. The lower the Corey oil exponent, the more favourable the recovery versus time (Hagoort, 1980):

$$N_p = 1-(1-1/no).\left(\frac{1}{no.k_{ro}^0 t_D}\right)^{\frac{1}{no-1}} \quad \text{Equation 4}$$

This scatter in curvature of oil relative permeability curves will then result in significant uncertainties in forecast of field reserves. In order to reduce these uncertainties, it is necessary to be able to assign the different Kr curves to dedicated zones within the reservoir. Then, seeking relationships between gas/oil

relative permeability curves and other rock characteristics is required to correctly populate the reservoir model with appropriate Kr curves.

SEEKING RESERVOIR TRENDS :

Attempts were made to correlate the oil Corey exponent or the oil saturation at different Krog values with either porosity, permeability or initial water saturations. These parameters are often used in empirical correlations (Hornarpour, 1982 ; Gerauld, 1996 ; Hamon, 1997). For fields A and B, there was no clear trend within the investigated range (porosity ranges from 20% to 37%, permeability ranges from 45 mD to 9D, initial water saturation ranges from 0.07 to 0.35).

Quantitative connection between textural and petrophysical properties :

The influence of texture on porosity and permeability of unconsolidated sands has been extensively studied (Fraser, 1935 ; Kozeny, 1927 ; Carman ; 1937 ; Morrow, 1969 ; Berg, 1970 ; Beard, 1973 ; Panda, 1994). These studies highlighted empirical relationships between porosity, permeability and some key features of the particle-size distribution, such as mean or median grain size, clay fraction or sorting coefficients. The number of equations relating petrophysical and textural properties and the number of adjustable parameters usually required for each equation illustrate that there is not a unique predictor (Nelson, 1994). Moreover, predictive algorithms which succeed in describing relationships for artificially mixed, packed sands, simple binary mixtures may fail to account for more complex reservoir unconsolidated sands.

When reservoir cores are available, it is worthwhile constructing a data base including both petrophysical and textural measurements and look for relationships between parameters. Such a statistically based model will be unique to the reservoir for which it is developed. Such an approach has been carried out for fields A and B.

For each poroperm or coreflood sample, porosity, permeability, grain density measurements, quantitative mineralogy and laser particle size analysis were performed. Several hundreds of measurements were then available for Fields A and B.

Statistical analysis of poroperm data evidenced some clear trends between petrophysical and textural properties: porosity and median grain size, fraction of clay+mica for instance. These results prompted us to check relationships between two-phase and textural properties.

Quantitative connection between textural and two-phase flow properties :

Figure 7 shows a significant relationship between the Corey oil exponent and the sorting coefficient. Figure 8 illustrates the trend between the sorting coefficient (or the presence of very coarse grains) and the residual oil saturation (@Krog=10^{-5}).

Well-sorted sands show very low residual oil saturation ($0. < Sorg < 0.05$) and favourable krog(Sg) curves ($3.7 < no < 4.7$). Poorly-sorted sands show larger residual oil saturation ($Sorg \sim 0.15$) and pessimistic krog(Sg) curves ($6 < no < 6.5$).

Figures 7 and 8 highlight the most significant relationships between textural properties and gas/oil relative permeability curves for fields A and B: the oil relative permeability is mainly controlled by grain size sorting (or the presence of very coarse grains): well-sorted sands have high recovery efficiency, more poorly sorted sands have lower recovery efficiency. Using equation 4 would show a large difference in microscopic recovery curve between well-sorted and poorly sorted sands for the gravity-drainage process.

The pore-size distribution should impact relative permeability rather than the grain-size distribution. However for unconsolidated sands, classical techniques to get insights into pore network are rather

unsuccessful. On the other hand, grain-size distribution can be routinely obtained on a foot basis and seems to capture indirectly some clues of the pore-size distribution.

These results are in agreement with recent studies which try to relate lithology and two-phase properties. Both water-oil (Coskun, 1993) and gas-oil displacements (Jerauld, 1996) illustrate the idea that sorting might be a key parameter of the microscopic recovery efficiency in strongly-wetted conditions.

Such a relationship between textural properties and relative permeability curves can be used to:

- Assign gas/oil relative permeability curves to a fine grid reservoir model,
- Choose the appropriate Kr curve if a dominant facies needs to be selected for model simplification,
- Reduce uncertainties in reserves forecast,

ASSIGNING GAS/OIL RELATIVE PERMEABILITY CURVES TO THE RESERVOIR MODEL :

On the field study example, the reservoir modelling is based on the mapping of Architectural Elements (AE). The AEs are defined referring simultaneously to sedimentological, lithological, textural, seismic and reservoir concepts and aiming at grouping, within an AE, rock volumes that share similar reservoir characteristics at simulation scale (200 x 200 x 5 m cells). The mapping is based on the observation of seismic facies. Each seismic facies is associated with a conceptual deposition environment based on well calibration (core and logs) and purely seismic characteristics (chaotic content, differential compaction, neighboring facies, etc..). Textural data is drawn from comparison to other fields and outcrops. Petrophysical data is derived from laboratory measurements.

Based on the core descriptions, it was found that only one core-defined lithology (medium grained sands) makes up most of the net thickness. Therefore, all AEs were built using only two core-defined lithologies : medium grained sands and shales.

Nevertheless grain size analysis on plugs shows that different lithological sub categories can be differentiated by their grain size and sorting, in the various sedimentological environments associated with each AE. The correlation found between grain size distribution and the shape of the oil relative permeability and residual saturations was therefore used to assign gas / oil relative permeability to the AEs within the 3D reservoir model. Two different gas / oil relative permeability curves are used in the 3D reservoir model, corresponding either to very well sorted sands (the most optimistic one for gas injection efficiency), or to poorly sorted sands (the most pessimistic one) : see figure 9. It was verified during the modelling process that pseudo Kr were not necessary for any AE in the gridding configuration used.

In order to evaluate the maximum sensitivity of gas injection efficiency to the relative permeability, and therefore to compare the results to a water injection scenario, two dynamic simulations were performed by assigning to all Architectural Elements the same gas/oil relative permeability, either the most pessimistic one, or the most optimistic one.
This results in a difference in term of reserves of about 14%.

CONCLUSIONS:

The following conclusions were drawn from this study on gas/oil relative permeability curves on unconsolidated, highly permeable, massive turbidite sands from deep water reservoirs:

1. CT proved to be a very useful tool in delineating severely disturbed, layered, laminated or coarse gravel sections for sample selection but the detection of slightly deconsolidated zones from CT images is rather subjective. A combination of three types of information was used to disregard heterogeneous samples : 1) Brine/brine tracer flow experiments, 2) qualitative CT scans inspection, 3) 1D X-Ray or Gamma-Ray profiles. This approach was very successful to resolve small-scale channels to flow.

2. Miscible flow simulation combined with heterogeneity geometry from CT scan was successfully used to estimate the permeability contrast within the core sample.
3. Multi-rate gas floods were performed with several advantages : the initial part of the gas flood experiment is carried out at relatively low flow rates but further changes in the balance between viscous and capillary forces are an advantage for the simultaneous determination of Kr and Pc curves. Finally, the last step at a high differential pressure ensures that the capillary end-effect has been minimised
4. Most of the gas core floods resulted in a break in the log/log plot of krog(So) at low oil saturations,
   - In the high and medium oil saturation range, Krog(So) is best fitted by : $Krog(S_o) \propto S_{oD}^{no}$ with $3.7 < no < 6.5$
   - In the low oil saturation range, Krog(So) is best fitted by : $Krog(S_o) \propto S_{oD}^{no}$ with $1.5 < no < 2.5$
5. This shape of the oil relative permeability might be ascribed to the change from bulk flow to film flow for spreading oils in three-phase conditions.
6. Experimental results show that most of the Krog curves cannot be correctly represented by a Corey form with a single-adjustable parameter. For the least squares optimisation, representation of Kr curves using spline functions adds the required flexibility to capture this key behaviour.
7. A large scatter in the curvature of oil relative permeability curves was evidenced for fields A and B with Corey exponent ranging from 3.7 to 6.5. Grain size analysis proved to be the most useful information to explain this scatter and to relate lithology to relative permeability.
8. A significant correlation between textural properties and unconsolidated gas/oil relative permeability curves was found: the oil relative permeability is mainly controlled by grain size sorting. Well-sorted sands show very low residual oil saturation and favourable krog(Sg) curves. Poorly-sorted sands show larger residual oil saturation and pessimistic krog(Sg) curves.
9. Relationship between the sorting of the grain size distribution and Krog curve was used to populate 3D reservoir models. Production forecasts showed a significant sensitivity of reserves to this relationship.

REFERENCES :

- Bahralolom, I.M. ; Heller, J.P : " Influence of Small-Scale Heterogeneities on Miscible Corefloods " SPE 24113, 1992 SPE/DOE Symposium on Enhanced Oil Recovery, Tulsa, USA
- Beard, D.C. ; Weyl, P.K. : " Influence of Texture on Porosity and Permeability of Unconsolidated sands " The American Association of Petroleum Geologists Bulletin, Feb. 1973
- Berg R.R. : " Method for determining Permeability from Reservoir Rocks Properties " GCAGS Transactions, v. 20 ; 1970
- Carman, P.C. : " Fluid flow through granular beds " Transactions of Institut of Chemical Engineering, London, 1937
- Chatzis I., Kantzas, A. : " On the investigation of Gravity Assisted Inert Gas Injection using Micromodels, Long Berea Cores and Computed Assisted Tomography " SPE 18284, 1988 SPE ATCE, Houston
- Chavent G., Cohen, G. : " Determination of Relative Permeabilities and Capillary pressures by an automatic Adjustment Method " SPE 9237, 1980 ATCE, Dallas, USA
- Coskun, S.B.; Wardlaw, N.C.: " Effects of composition, texture, and diagenesis on porosity, permeability and oil recovery in a sandstone reservoir" Journal of Petroleum science and Engineering, 1993
- Dauba, C. ; Hamon, G. : " Stochastic Description of Experimental 3D Permeability Fields in vuggy reservoir Cores " SCA 9828, 1998 Symposium of the Society of Core Analysts, The Hague, NL.
- Dauba, C. ; Hamon, G. : " Application of Miscible Displacement to identify Along-Axis Heterogeneities on Core Flood Samples " SCA 9933, 1999 Symposium of the Society of Core Analysts, Golden, USA

- Delclaud, J : " New results on the Displacement of a Fluid by another in Porous Media " SPE 4103, 1972, San Antonio, USA
- Delclaud, J. : " Etude du déplacement de l'huile par le gaz " Revue IFP, 1974 (In French)
- Delclaud, J. ; Rochon, J : " Investigation of Gas/oil Relative Permeabilities : High-Permeability Oil Reservoir Application " SPE 16966, 1987 ATCE, Dallas, USA
- DeZabala, EF ; Kamath, J. : " Laboratory Evaluation of Waterflood Behavior of Vugular Carbonates " SPE 30780, 1995 ATCE, Dallas, USA
- DiCarlo, D, Sahni, A : " The effect of Wettability on Three-Phase Relative Permeability " SPE 49317, SPE ATCE, New Orleans, USA, Sept. 1998
- Dumoré J.M : " Drainage Capillary Pressure Functions and the influence of connate water " SPEJ, 1974
- Fenwick, D.H. ; Blunt, M : " Network Modelling of Three-Phase Flow in Porous Media " SPEJ, 1998
- Fraser, H.J ; Graton, L.C. : " Systematic Packing of Spheres - with Particular Relation to Porosity and Permeability " Journal of Geology, Nov. 1935
- Gerauld, G.R. : " Gas/oil Relative Permeability of Prudhoe Bay " SPE 35718, Anchorage, USA, 1996
- Hagoort, J. : " Oil Recovery by Gravity Drainage " SPEJ, June 1980
- Hamon, G. ; Vidal, J. : " Scaling-Up the capillary Imbibition Process from Laboratory Experiments on Homogeneous and Heterogeneous Samples " SPE 15852, 1986 Europec Conference, London, UK
- Hamon, G. ; Pellerin, F.M. : " Evidencing Capillary Pressure and Relative Permeability Trends for Reservoir Simulation " SPE 38898, 1997 ATCE, San Antonio, USA
- Hornarpour, M. ; Koederitz, L.F : " Empirical Equations for Estimating Two-Phase Relative Permeability in Consolidated Rocks " JPT, Dec. 1982
- Hornarpour, M; Mahmood, S.M.: " Relative-Permeability Measurements, An Overview" JPT, August 1988
- Huang, Y. ; Ringrose, P.S. : " Waterflood Displacement Mechanisms in a Laminated Rock Slab : Validation of Predicted Capillary Trapping Mechanisms " SPE 28942, 1994 ATCE, New Orleans, USA
- Jennings, J.W. ; McGregor, D.S : " Simultaneous Determination of Capillary Pressure and relative Permeability by Automatic History Matching " SPEFE, June 1988
- Kantzas, A.,Chatzis, A. : " Enhanced Oil Recovery by Inert Gas Injection " SPE/DOE 17379, 1988 SPE/DOE EOR Symposium, Tulsa
- Kantzas, A.,Chatzis, A. : " Mechanisms of Capillary Displacements of Oil by Gravity Assisted Inert Gas Injection " SPE 17506, 1988 Rocky Mountain Meeting, Casper
- Kerig, P.D. ; Watson, A.T. : " Relative-Permeability Estimation from Displacement Experiments : An error Analysis " SPERE, March 1986
- Kohhedee, J.A. : " Simultaneous Determination of Capillary Pressure and Relative Permeability of a Displaced Phase " SPE 28827 , 1994 Europec Conference, London, UK
- Krumbein,W.C. ; Monk, G.D. ; " Permeability as a Function of the Size Parameters of Unconsolidated Sands " AIME Transactions, 1942, v. 151
- Nelson, P.H. : " Permeability-Porosity Relationships in Sedimentary Rocks " The Log Analyst, May 1994
- Nordtvedt, J.E. ; Urkedal, H ; " Estimation of Relative Permeability and Capillary Pressure functions Using Transient and Equilibrium Data from Steady-State Experiments " SCA 9418, 1994 Symposium of the Society of Core Analysts, Stavanger, Norway
- Morrow, N. ; Huppler, J. : " Porosity and Permeability of unconsolidated, Upper Miocene sands from Grain-size Analysis " Journal of Sedimentary Petrology, 1969
- Panda, M.N. ; Lake, L.W. : " Estimation of Single-phase Permeability from Parameters of Particle-Size Distribution " AAPG Bulletin, V. 78, 1994
- Richmond, P.C. ; Watson, A.T. : " Estimation of Multiphase Flow Functions from Displacements experiments " SPERE, February 1990

- Saad, N., Cullick, A.S. : " Immiscible Displacement Mechanisms and Scale-Up in the Presence of Small Scale Heterogeneities " SPE 30779, 1995 ATCE, Dallas, USA
- Sahni, A., Burger, J. : " Measurements of three Phase Relative Permeability during Gravity Drainage using CT scanning " SPE 39655, SPE/DOE IOR Symposium, Tulsa, USA, April 1998
- Sultan, A.J ; " Simulation of Matched Viscosity Miscible Displacement in a Heterogeneous Porous Medium " MS Thesis, New Mexico Institute of Mining and Technology, Socorro, USA, 1987
- Sylte, A ; Mannseth, T. : " Relative Permeability and Capillary Pressure : Effects of Rock Heterogeneity " Paper SCA 9808, SCA Symposium, The Hague, 1998
- Ucan, S ; Civan, F : " Simulated Annealing for Relative Permeability and Capillary Pressure from Unsteady-State Non-Darcy Displacement " SPE 26670, 1993 ATCE, Houston, USA
- Ucan, S ; Civan, F : " Uniqueness and Simultaneous Predictability of Relative Permeability and Capillary Pressure by Discrete and Continuous Means " JCPT, April 1997
- Vizika O., Lombard, JM : " Wettability and Spreading : two key parameters in oil Recovery with Three-Phase Gravity Drainage " SPERE, Feb. 1996

AKNOWLEDGMENTS :

The authors thank Elf Exploration Production for permission to publish this study. We thank P. Clament, P. Ducarme, P. Maurin for their contribution to the experimental work. Helpful discussions with T. Fincham of Elf Geoscience Research Center, and contributions of C. Dauba, J. Barro, B. Levallois and F.M. Pellerin are gratefully acknowledged.

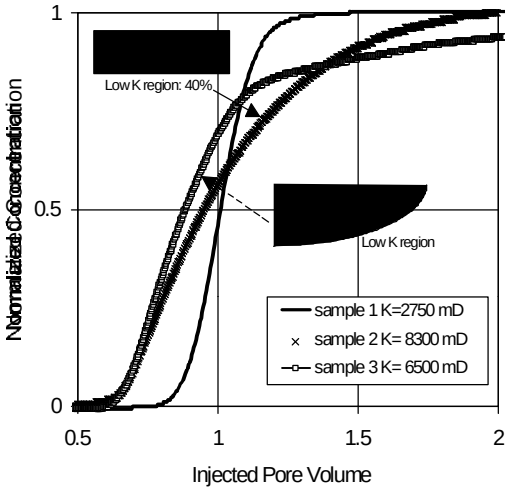

Figure 1 : Brine/Brine Tracer experiment

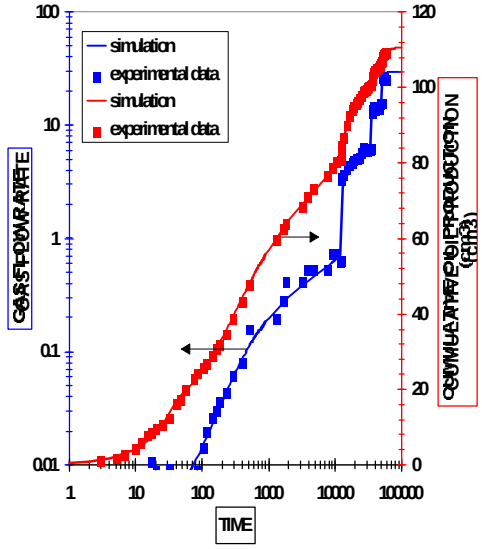

Figure 2 : Multi-rate gas flood test

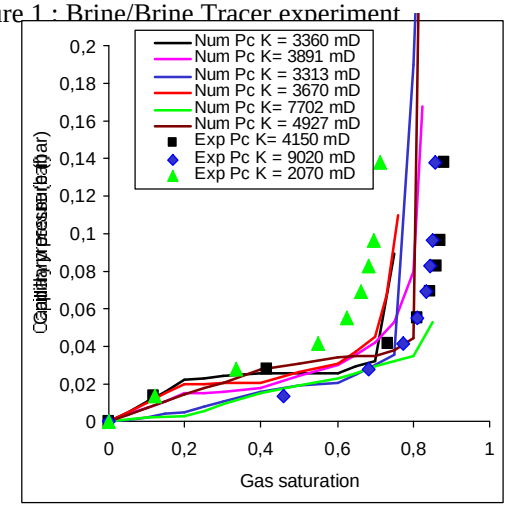

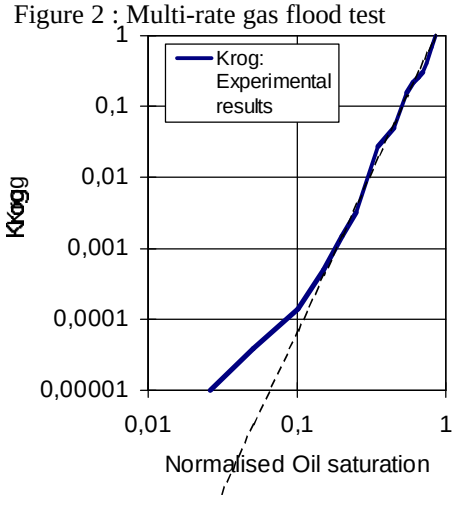

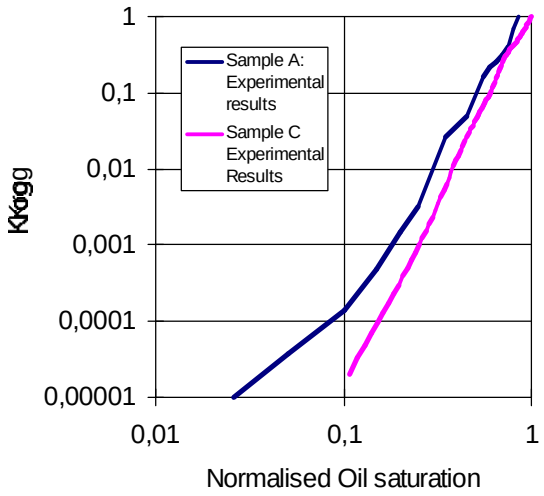

Figure 5 : Two different behaviours in log/log plot of Krog curves

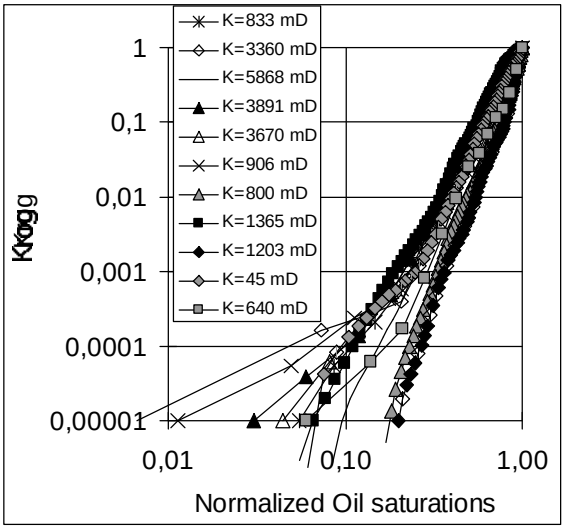

Figure 6 : Scatter in Krog curves for fields A and B

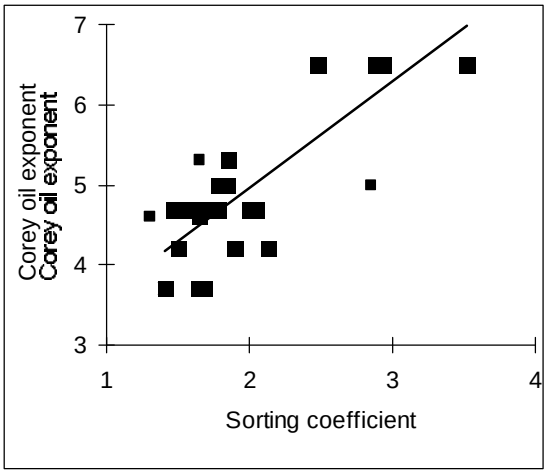

Figure 7 : Relationship between Corey oil exponent and sorting coefficient

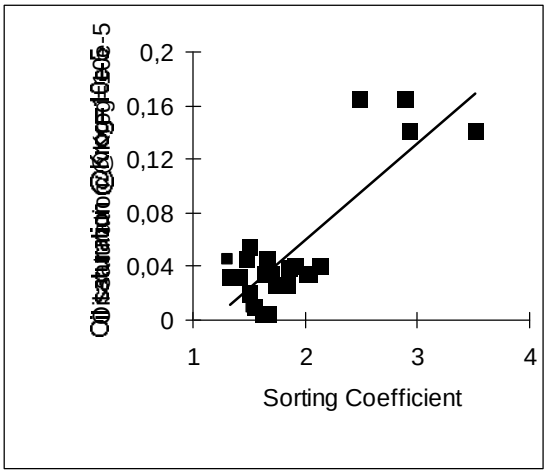

Figure 8 : Relationship between residual oil saturation and sorting coefficient

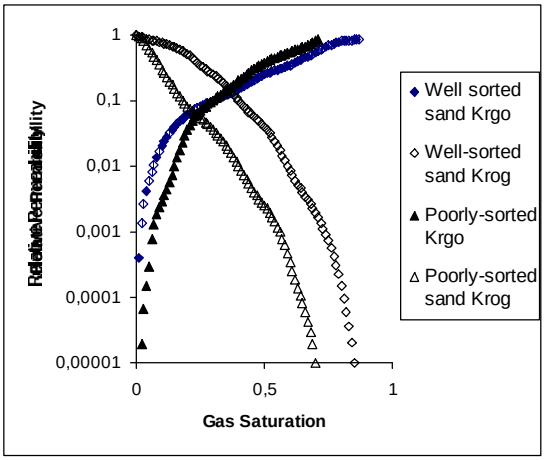

Figure 9 : Gas/oil relative permeability